© Universiti Tun Hussein Onn Malaysia Publisher's Office

IJIE

http://penerbit.uthm.edu.my/ojs/index.php/ijie
ISSN : 2229-838X e-ISSN : 2600-7916

The International Journal of Integrated Engineering

Comparison Study on Pinch-Hitting Vibration Signal Analysis for Automotive Bearing: I-Kaz^{TM} and I-Kaz 3D

A. Othman[1*], H. Hamid[1], M. A. F. Ahmad[2], M. Z. Nuawi[2]

[1]Universiti Kuala Lumpur MFI, Water & Energy Section,
Seksyen 14 Jalan Teras Jernang, Bandar Baru Bangi, 43650, Selangor, MALAYSIA

[2]Universiti Kebangsaan Malaysia, Department of Mechanical and Materials Engineering, Faculty of Engineering and Built Environment, Universiti Kebangsaan Malaysia, 43600 Bangi, Selangor, MALAYSIA

*Corresponding Author

DOI: https://doi.org/10.30880/ijie.2023.15.05.027
Received 1 August 2023; Accepted 15 August 2023; Available online 19 October 2023

Abstract: Rotating machines are now an essential part of the automotive industry. Meanwhile, a bearing is playing the most important component of rotating machinery. To sustain the system's smooth running, maintenance methods such as preventive maintenance, breakdown maintenance, and predictive maintenance are used. Under preventive maintenance, vibration analysis is used to diagnose machines bearing faults. The main objective is to recognize bearing defects in a mechanical device by acquiring signals from the bearing using data acquisition hardware. This analysis is conducted under various load torque conditions, speeds, and defect types. A modular hardware configuration consisting of an accelerometer acquires the vibration signal. The signals are analyzed by using I-kaz^{TM} and I-kaz 3D signal analysis and its main objective is to observe the degree of dispersion data from its mean point. This analysis resolves the issues associated with time domain analysis. This pinch-hitting analysis research was conducted in two stages. The first stage is an experimental process that uses 3 types of bearings, the healthy (BL), inner race fault (IRF), and defect at outer race (ORF) bearing on the Machine Fault Simulator and forces with a different type of speed (1000, 1500 and 2500 rpm) and load variation (0.0564, 0.564 and 1.1298 N-m). In the second stage, computing the coefficient value and plots of signal's I-kaz^{TM} and I-kaz 3D based on the bearings type were done accordingly. As a result, the analysis for detecting inner race fault, the deviation percentage averages calculation obtained the I-kaz^{TM} coefficient shows a better result with 96.86% by comparing to the I-kaz 3D that achieves 94.20%. Similarly, for the outer race defect, I-kaz^{TM} lead with 65.40% compared to I-kaz 3D with only 54.82%.

Keywords: I-kaz, defect bearing, vibration, accelerometer, condition monitoring

1. Introduction

It has been acknowledged that every rotating machine or a moving part of every vehicle that makes it something to move or accelerate is widely dependent on the rolling action of rollers that we call bearings. In many industrial applications, the bearing is useful to ensure very minimum friction between two major components names as stator and rotor from the forced motion to each other. To avoid any serious damage that happens to machines from unexpected failure, many industries have given more attention to condition monitoring (CM) techniques by ensuring proper operation of mechanical equipment, especially the bearings. The bearing is critical to achieving an optimized and smooth machinery operation despite being frequently forced by heavy loads. The most common type of faulty bearing that is difficult to avoid in operating conditions is a scratch on the surface caused by repetitive shaft loading and surface fatigue [1]. Thus, the biggest challenge in detecting a bearing failure is to identify if there is a surface defect on the bearing before it turns more severe and catastrophic to the whole system. CM focuses on a three-stage development process, firstly data

*Corresponding author: affandy@unikl.edu.my

acquisition and storing, secondly data processing and feature extracting, and finally results analysis and recognized conditions. Different methods are used for the acquisition of information; the most popular method was vibration. Most other techniques were acoustic emissions, currents, lubricant conditions, strain, wear, rotor-to-stator rubbing, motor current stator, and debris analysis [2]. An accelerometer is always to be used as the vibration data acquisition technique since it is most suited and effective for bearing. It has been widely employed in many industries used to extract the measured information before any prediction can be made to the respected tested systems. The installation is handy and carries a wealth of data signal information. However, not everyone could read and translate the data for a given signal. The extracted data can be examined into three work processes, namely time domain, frequency domain, and time-frequency domain analysis, which make up most of these approaches. Time domain analysis computes the statistical characteristics of signals, including the mean, peak-to-peak, variance, kurtosis, skewness, crest, impulse, margin, etc [3].

Statistics is a mathematical science that deals with data collection, analysis, interpretation, and presentation. These methods are used in a wide spectrum of issues to assist researchers in identifying, studying, and solving any difficult problems. From an engineering perspective, statistics allow decision-makers to make greater awareness and better decisions in doubtful situations. Descriptive statistics are statistical methods that summarize or describe a collection of data analytically or visually, whereas inferential statistics model the pattern in the data in a way to considering the unpredictability of the observations. Many researchers have proven useful techniques of pattern recognition to classify data based on statistical information. Kasim, Mohamed, and Nuawi [4] developed a Z-Rotation method based on the variance of a signal element dispersion around its mean centroid. It detects inferences and is expected to be more sensitive to variations in signal amplitude and anomalies. The technique exhibits data patterns in defining the randomness of non-stationary time series data. Various methods of analyzing the statistical properties of signals have been used, but in condition monitoring applications, the flexibility of the chosen method comes first. According to [5], outliers in real-world signals can shift the actual value of mean and variance, making signal classification unreliable. The statistical characteristics reflect the trend of time series signals, that only include the standard frequency band. However, in the cases of non-stationary machine signals, it was made these features are insufficient. Towards these drawbacks, it would be useful to develop an option method for improvements. The novel technique known as the Integrated kurtosis-based algorithm for the Z-notch filter (I-kaz^{TM}) can contribute to an effective condition monitoring system effectively and reliably.

1.1 I-Kaz

Targeting the modulation image and morphology pattern for distribution frequency points of bearing fault vibration signals, the goal of the I-kaz analysis is to determine the level of information data to its mean point for a dynamic signal. Both graphical and derivable statistics were utilized in this method. The I-kaz coefficient, Z^{∞}, is the numerical descriptor, and its value is parallel by three-dimensional graphical summarizations of frequency occurrence [6]. Furthermore, I-kaz can classify inferential statistics by showing a model pattern in the data, considering inconsistency, and drawing inferences. These two parameters are hugely important in estimating and forecasts for the next level of analysis.

1.2 I-Kaz^{TM}

The I-kaz^{TM} algorithm flowchart is presented in Figure 1. As mentioned earlier, the main concept of I-kaz^{TM} development is based on data scattering from its centroid. The representation is based on three-dimensional spaces, to generalize to higher dimensions. The first method from the flowchart is decomposition into three frequency ranges from a time domain signal. Every three axes will be named Low frequency (LF), High frequency (HF), and Very high frequency (VF) as the representation of three-dimensional scattering data. From the right-hand rules in Figure 2, the three-dimensional axis represents the data captured from the tri-axial accelerometer in detecting vibration output from the measured bearing.

- x-axis: LF scale from 0 - 0.25 fmax
- y-axis: HF scale of 0.25 fmax - 0.5 fmax
- z-axis: VF scale above 0.5 fmax

To quantify scattering in a data distribution, the variance value of every frequency scale which is σ_L^2, σ_H^2 and σ_V^2 is computed as in Eq.1. The goal is to calculate the average magnitude deviation of instantaneous points from the mean value. Thus, the I-kaz^{TM} coefficient Z^{∞} can be simplified and written as Eq.2.

$$\sigma_L^2 = \frac{\sum_{i=1}^{N}(x_i^L - \mu_L)^2}{n} \; ; \; \sigma_H^2 = \frac{\sum_{i=1}^{N}(x_i^H - \mu_H)^2}{n} \; ; \; \sigma_V^2 = \frac{\sum_{i=1}^{N}(x_i^V - \mu_V)^2}{n} \quad (1)$$

$$Z^{\infty} = \sqrt{(\sigma_L^2)^2 + (\sigma_H^2)^2 + (\sigma_V^2)^2} \quad (2)$$

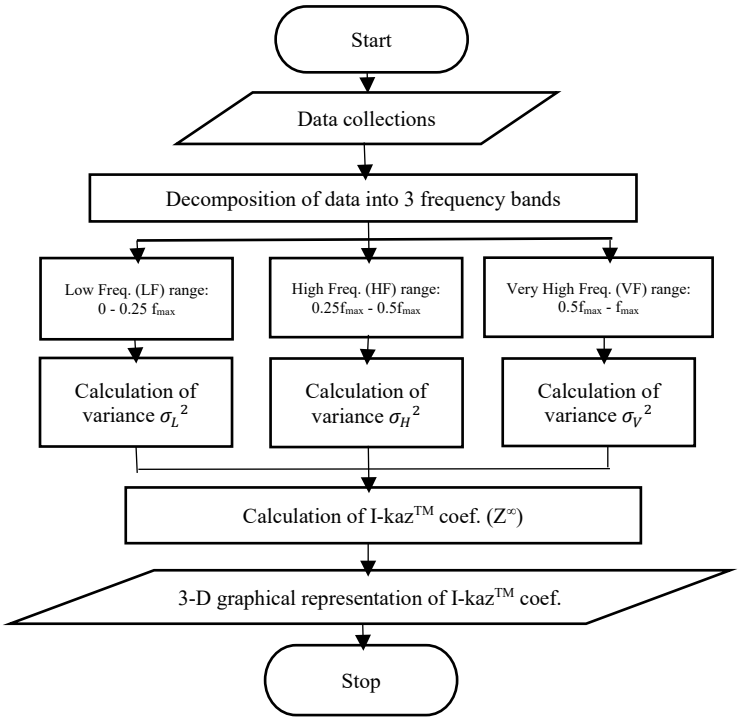

Fig. 1 - I-kaz™ algorithm

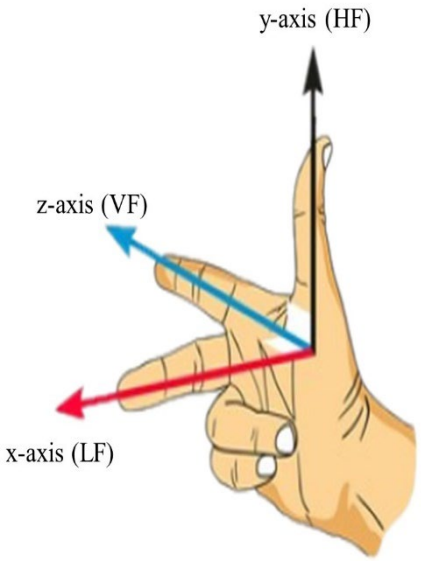

Fig. 2 - Direction axis of each frequency band

1.3 I-Kaz 3D

With a similar objective to I-kaz™, the I-kaz 3D more focusing in measuring the degree of scattering for three axial signals. The algorithm of this technique skipped on the process which is decomposing the axis signal into 3 different frequency bands. The reason is that each data captured by the three different axes of tri-axial accelerometers will be directly assigned as LF, HF, and VF for the axis x, y, and z from accelerometer vibration data respectively. The computational descriptor of I-kaz 3D is the coefficient value which is synchronized by the I-kaz 3D graphical summarizations of magnitude distribution. The I-kaz 3D coefficient can be computed using Eq. 3.

$$Z_3^{\infty} = \frac{1}{n}\sqrt{K_1 * {s_1}^4 + K_2 * {s_2}^4 + K_3 * {s_3}^4} \quad (3)$$

Whereas K_1, K_2, and K_3 are kurtosis and s_1, s_2, and s_3 are standard deviations for each channel respectively. Furthermore, [7], have proven that I-kaz 3D can observe a minor bearing defect through this statistical analysis technique. However, the main challenge of the I-kaz 3D method is to place the measured sensor to capture the x,y, and z axes. According to [8] the I-kaz 3D gives better scatterings, indicating that the values of the I-kaz 3D coefficient (Z^{∞}_{3D}) were getting higher and very useful in predicting and determining whole-body vibration (WBV) exposure in the truck driver's seat.

2. Experimental Setup and Measurements

The test rig used in the present work consists of 1 Hp, 3600 rpm, Marathon, three-phase induction motor. It is equipped with an LCD, tachometer, and one pulse per revolution analog for data acquisition purposes. The test bearing is in split bracket housing with five mounting positions for accelerometer installations. Vibration isolation rubber mounts and base stiffener were placed under the test rig to reduce the vibration transmission from the ground to the test bearing. To get a vibration response of faulty rolling element bearing, three types of ER12KCL (Rexnord) 3/4" unmounted ball bearing, standard duty, set screw locking, and single lip contact seal were tested. The specifications are listed as follows, the balls are 8, and the diameter of the ball is 7.9375mm. The angle of the contact bearing is 0° and the pitch diameter is 38.15 mm. Two of the three bearings were artificially defective with one of them on its inner race part and the other one on its outer race. The defect on the bearing is a dent and the diameter of the dent is about 3mm and 0.5mm deep. Figure 3a and 3b show the defect of the inner race and outer race respectively. The remaining healthy bearing will be referred to as baseline vibration data in this study analysis. Meanwhile, Figure 4 shows the schematic diagram of the experimental setup for the acquisition of data vibration study.

The vibration signal from the bearing was acquired by using a triaxial accelerometer brand Rion with type number PV-93. The accelerometer was mounted on external bearing housing with the aid of screw-type mounting. The charge sensitivity of the accelerometer is 0.831pC or (m/s^2) or approximately equal to 100mV/g. These vibration signals were captured using the data acquisition module brand Measurement Computing series DT9837 and stored in the computer

for measurement analysis. Matlab software was used in this analysis study. Figure 5 shows the complete process of these vibration analysis studies. During the measurements process, three parameters of studies were decided to be addressed. First is the type of defective bearing, second is variation speed (RPM) and the third is a braking load torque that is applied to the bearing. From this study, three different speeds were chosen to be captured for the data collection which are 1000, 1500, and 2500 rpm. Additionally, the load variation was decided to be imposed on 0.0564, 0.564, and 1.1298 N-m. The main reason for these parameters' variation of speed (RPM) and load torque (N-m) was chosen, is to acquire a new indicator of defected bearing signal without having an additional sensor installed.

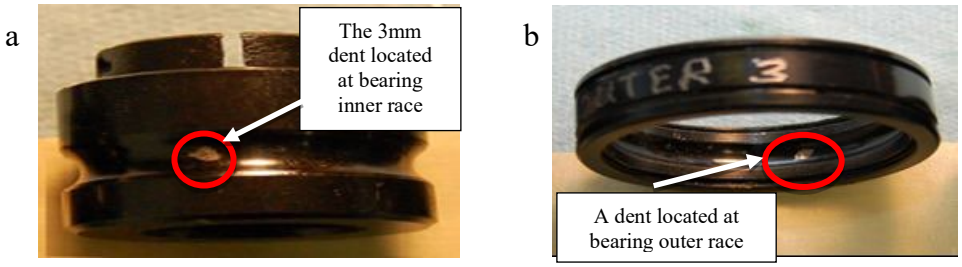

Fig. 3 - The location of bearing defect (a) inner race (IRF); (b) outer race (ORF)

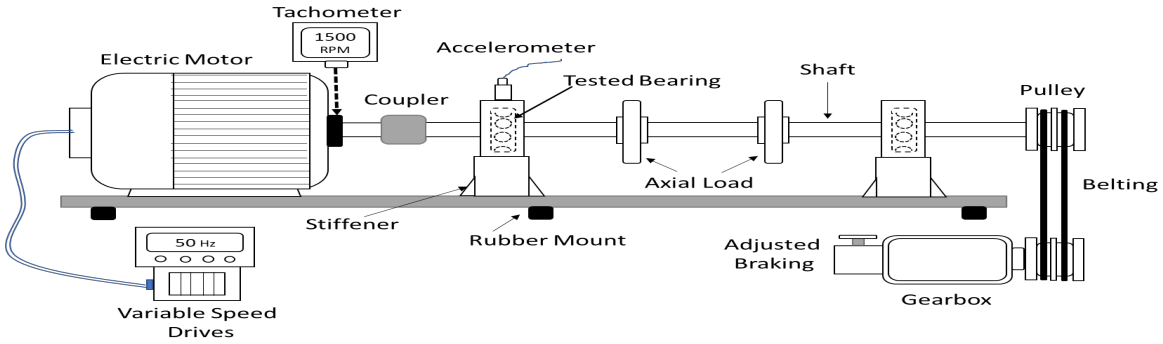

Fig. 4 - Experimental setup

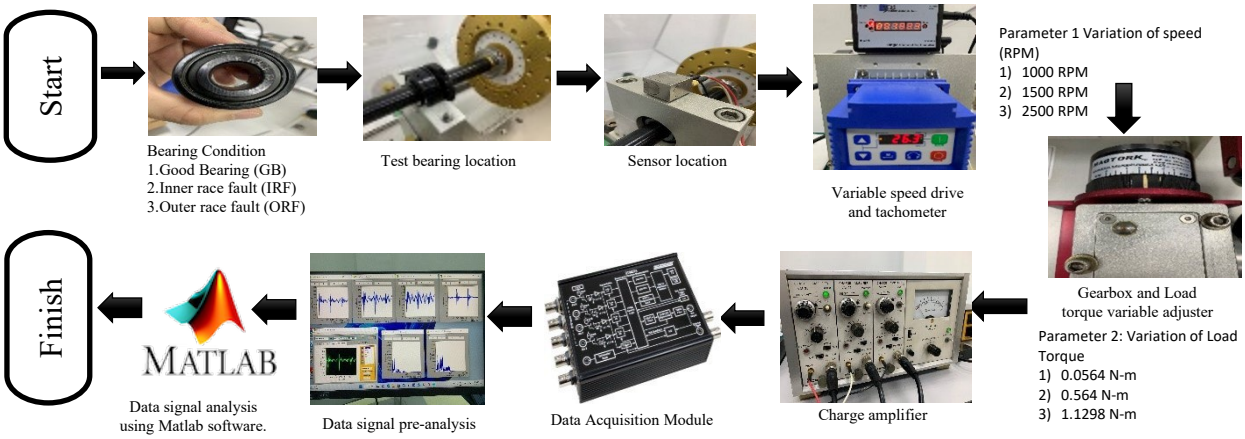

Fig. 5 - Research methodology

3. Results and Discussions

The following section shows the results from the analysis obtained from the Matlab platform. The I-kaz^{TM} for each axis and I-kaz 3D were plotted and calculated to study their reliability and performance in detecting the defect's bearings. All figures plotted in figure 6 to 17 is to observe the data scattering from its centroid. The main objective was to show that there is a difference in frequency pattern morphology between signal data from the healthy bearing and faulty bearing. From the scattering plot figures, it can show the output pattern signal varies proportional to the speed (RPM) and the load torque applied to the motor. For example, the data output from a good bearing as represented in Figure 6(a)-(d) with parameter speed 1000 rpm and load torque 0.0564 N-m has a bigger difference in terms of size by comparing to the output represented in Figure 7(a)-(d) with 2500 rpm and similar load torque was applied. But to compare the pattern of output size according to the variation of load with similar motor speed, it can be referred to figure 7(a)-(d) as compared

to figure 13(a)-(d). From this observation, it shows that there is a slight difference in pattern output according to the variation of load torque.

In the case of defect bearing IRF and ORF as shown in Figure 9 - 11, it was shown that the scattering data of the output signal was dispersed far away from its centroid, and the pattern was no longer intact like a ball shape (healthy bearing case). These results showed that the vibration signal produced by the faulty bearing can be detected by the accelerometer successfully. Figure 12 to 17 presents the data scattering of the output signal with the variation of load torque (N-m) applied to the bearing of the motor. The representation of I-kaz^{TM} and I-kaz 3D is shown in the following figures:

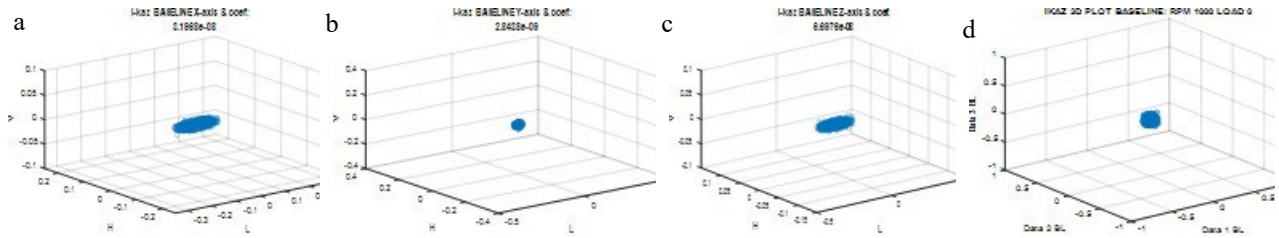

Fig. 6 - The representation of I-kaz^{TM} (a) x-axis; (b) y-axis; (c) z-axis, and; (d) I-kaz 3D for baseline or good bearing (BL) with parameter speed 1000 rpm and load 0.0564 N-m

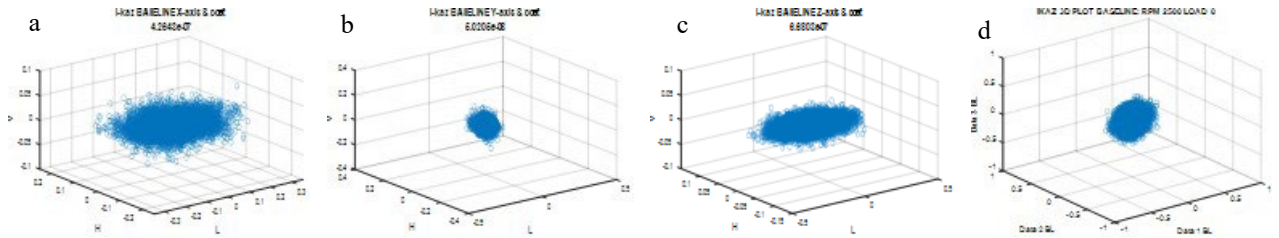

Fig. 7 - The representation of I-kaz^{TM} (a) x-axis; (b) y-axis; (c) z-axis, and; (d) I-kaz 3D for baseline or good bearing (BL) with parameter speed 2500 rpm and load 0.0564 N-m

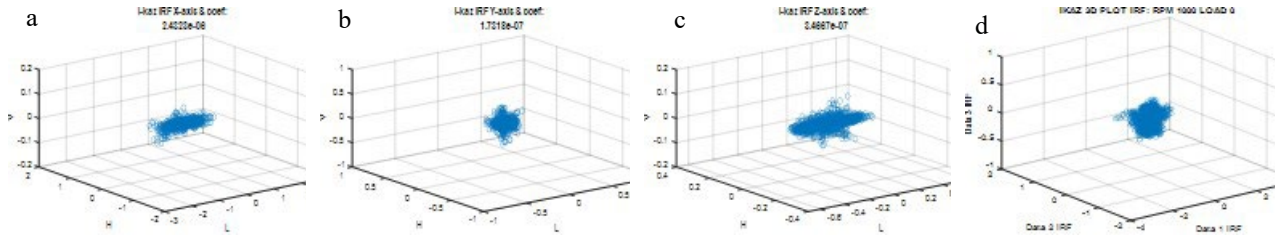

Fig. 8 - The representation of I-kaz^{TM} (a) x-axis; (b) y-axis; (c) z-axis, and; (d) I-kaz 3D for Inner race fault (IRF) with parameter speed 1000 rpm and load 0.0564 N-m

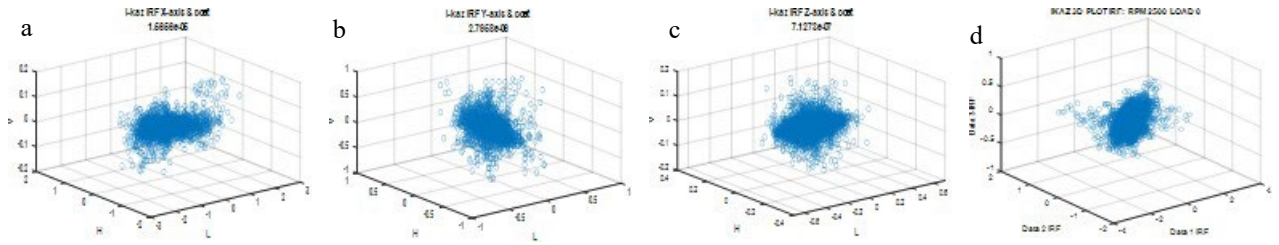

Fig. 9 - The representation of I-kaz^{TM} (a) x-axis; (b) y-axis; (c) z-axis, and; (d) I-kaz 3D for inner race fault (IRF) with parameter speed 2500 rpm and load 0.0564 N-m

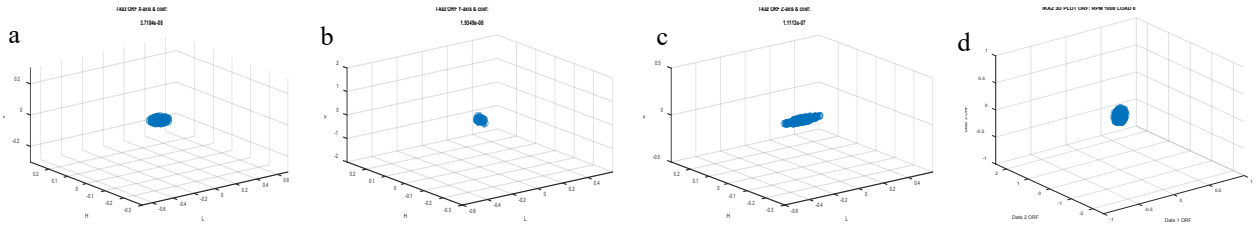

Fig. 10 - The representation of I-kaz^{TM} (a) x-axis; (b) y-axis; (c) z-axis, and; (d) I-kaz 3D for outer race fault (ORF) with parameter speed 1000 rpm and load 0.0564 N-m

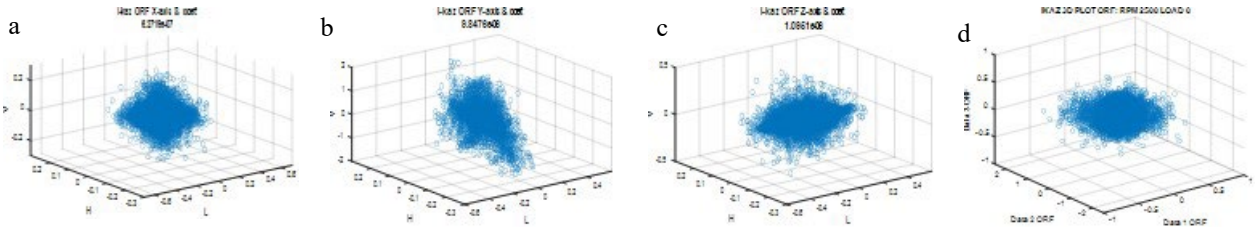

Fig. 11 - The representation of I-kaz^{TM} (a) x-axis; (b) y-axis; (c) z-axis, and; (d) I-kaz 3D for outer race fault (ORF) with parameter speed 2500 rpm and load 0.0564 N-m

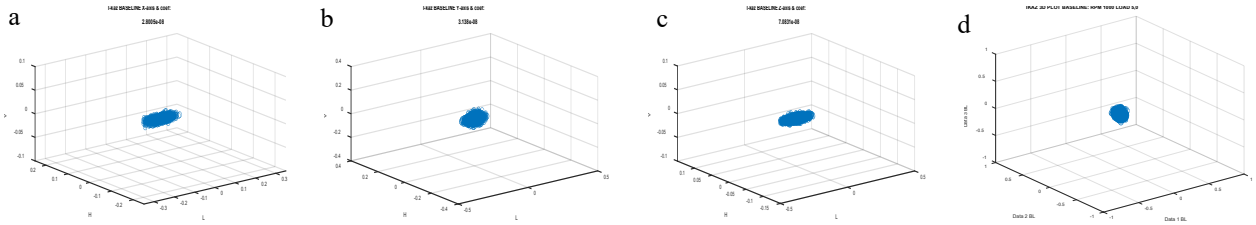

Fig. 12 - The representation of I-kaz^{TM} (a) x-axis; (b) y-axis; (c) z-axis, and; (d) I-kaz 3D for baseline or good bearing (BL) with parameter speed 1000 rpm and load 1.1298 N-m

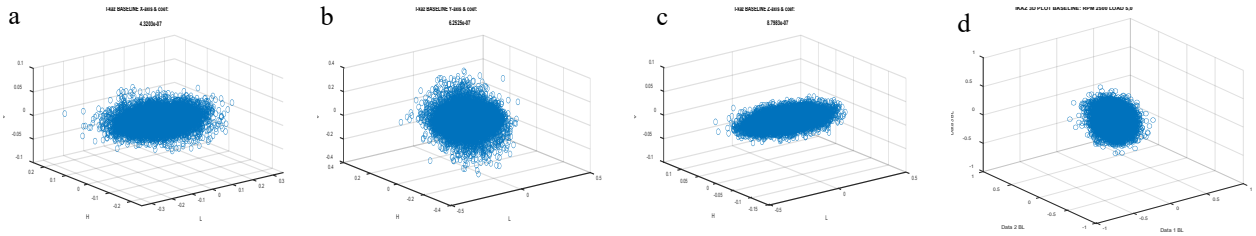

Fig. 13 - The representation of I-kaz^{TM} (a) x-axis; (b) y-axis; (c) z-axis, and; (d) I-kaz 3D for baseline or good bearing (BL) with parameter speed 2500 rpm and load 1.1298 N-m

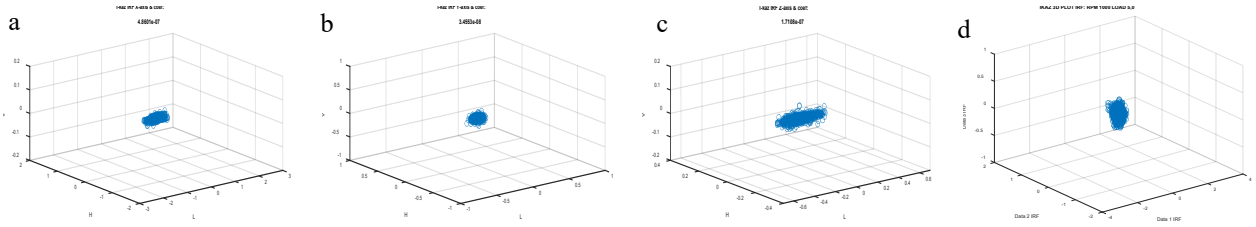

Fig. 14 - The representation of I-kaz^{TM} (a) x-axis; (b) y-axis; (c) z-axis, and; (d) I-kaz 3D for inner race fault (IRF) with parameter speed 1000 rpm and load 1.1298 N-m

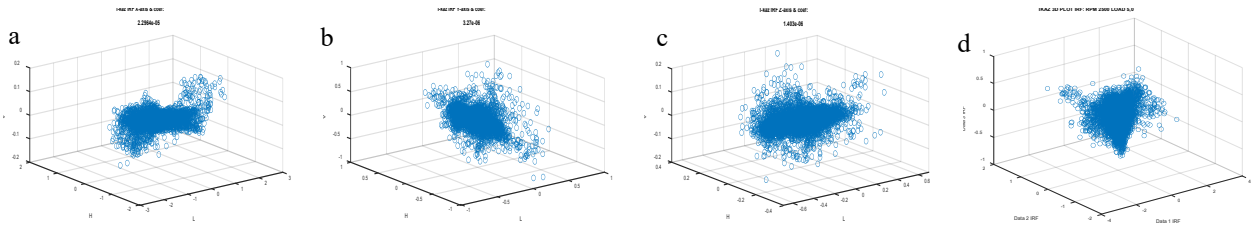

Fig. 15 - The representation of I-kaz^{TM} (a) x-axis; (b) y-axis; (c) z-axis, and; (d) I-kaz 3D for inner race fault (IRF) with parameter speed 2500 rpm and load 1.1298 N-m

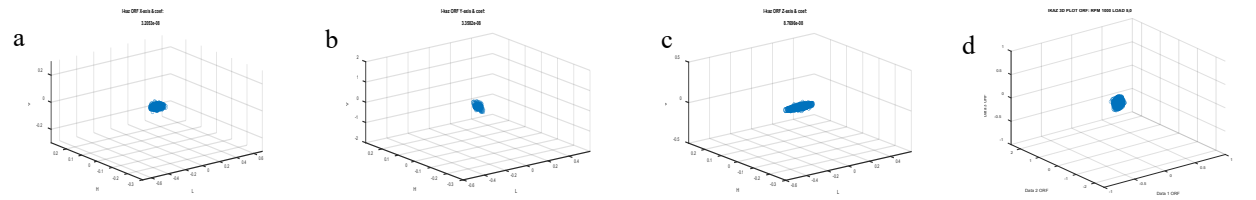

Fig. 16 - The representation of I-kaz^{TM} (a) x-axis; (b) y-axis; (c) z-axis, and; (d) I-kaz 3D for outer race fault (ORF) with parameter speed 1000 rpm and load 1.1298 N-m

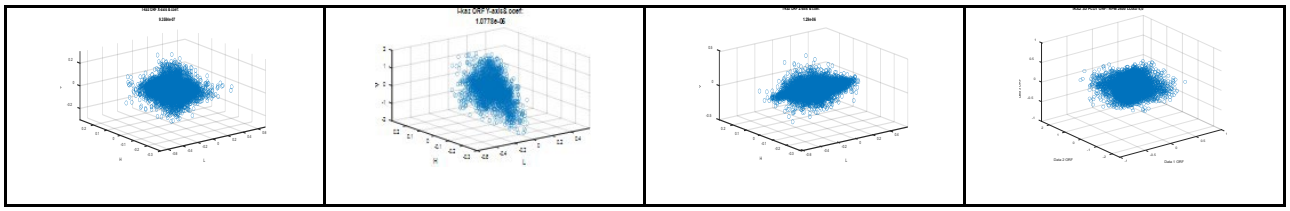

Fig. 17 - The representation of I-kaz^{TM} (a) x-axis; (b) y-axis; (c) z-axis, and; (d) I-kaz 3D for outer race fault (ORF) with parameter speed 2500 rpm and load 1.1298 N-m

The following tables show the summary of I-kaz^{TM} and I-kaz 3D coefficient calculated values.

Table 1 - I-kaz^{TM} coefficient for X-axis

Load (N-m)	Speed (rpm)	BL	IRF	ORF	Deviation BL-IRF	Deviation BL-ORF
0.0564	1000	3.19681E-08	2.43229E-06	3.71843E-08	98.69	14.03
0.0564	1500	1.25462E-07	1.22572E-06	1.31379E-07	89.76	4.50
0.0564	2500	4.26432E-07	1.56558E-05	6.27192E-07	97.28	32.01
0.564	1000	3.26058E-08	2.53242E-06	3.39942E-08	98.71	4.08
0.564	1500	8.00579E-08	5.08179E-06	1.14906E-07	98.42	30.33
0.564	2500	4.63898E-07	2.25812E-05	6.1671E-07	97.95	24.78
1.1298	1000	2.80049E-08	4.86008E-07	3.20534E-08	94.24	12.63
1.1298	1500	7.29216E-08	5.06762E-06	1.04215E-07	98.56	30.03
1.1298	2500	4.32031E-07	2.29635E-05	9.35841E-07	98.12	53.83
				Average:	96.86%	22.91%

Table 2 - I-kaz^{TM} coefficient for Y-axis

Load (N-m)	Speed (rpm)	BL	IRF	ORF	Deviation BL-IRF	Deviation BL-ORF
0.0564	1000	2.84377E-09	1.73182E-07	1.93493E-08	98.36	85.30
0.0564	1500	1.01215E-08	1.53547E-07	6.76281E-07	93.41	98.50
0.0564	2500	5.02051E-08	2.7958E-06	9.84765E-06	98.20	99.49
0.564	1000	3.43432E-08	2.80767E-07	3.5934E-08	87.77	4.43
0.564	1500	9.34532E-08	5.67877E-07	2.27594E-07	83.54	58.94
0.564	2500	6.394E-07	2.9872E-06	1.03468E-05	78.60	93.82
1.1298	1000	3.13803E-08	3.4553E-08	3.35824E-08	9.18	6.56
1.1298	1500	9.2153E-08	7.24713E-07	1.77181E-07	87.28	47.99
1.1298	2500	6.25249E-07	3.27002E-06	1.07785E-05	80.88	94.20
				Average:	79.69%	65.47%

Table 3 - I-kaz^{TM} coefficient for Z-axis

Load (N-m)	Speed (rpm)	BL	IRF	ORF	Deviation BL-IRF	Deviation BL-ORF
0.0564	1000	6.69757E-08	3.4667E-07	1.11131E-07	80.68	39.73
0.0564	1500	1.52234E-07	2.60046E-07	2.83953E-07	41.46	46.39
0.0564	2500	6.68029E-07	7.12728E-07	1.09507E-06	6.27	39.00
0.564	1000	8.44522E-08	7.15522E-07	1.19771E-07	88.20	29.49
0.564	1500	1.48945E-07	6.35378E-07	2.78268E-07	76.56	46.47
0.564	2500	8.85971E-07	1.63929E-06	1.25599E-06	45.95	29.46
1.1298	1000	7.08312E-08	1.71077E-07	8.76964E-08	58.60	19.23
1.1298	1500	1.2755E-07	5.95199E-07	2.49113E-07	78.57	48.80
1.1298	2500	8.79834E-07	1.40301E-06	1.29004E-06	37.29	31.80
				Average:	57.06%	36.71%

Table 4 - I-kaz 3D coefficient

Load (N-m)	Speed (rpm)	BL	IRF	ORF	Deviation BL-IRF	Deviation BL-ORF
0.0564	1000	7.6519E-08	2.9584E-06	1.2265E-07	97.41	37.61
0.0564	1500	2.1711E-07	1.6468E-06	8.0426E-07	86.82	73.00
0.0564	2500	8.9326E-07	2.2404E-05	1.0358E-05	96.01	91.38
0.564	1000	1.0343E-07	3.3194E-06	1.3300E-07	96.88	22.24
0.564	1500	2.3095E-07	6.9800E-06	4.0494E-07	96.69	42.97
0.564	2500	1.4718E-06	3.2412E-05	1.0850E-05	95.46	86.43
1.1298	1000	8.8547E-08	6.2718E-07	1.0315E-07	85.88	14.15
1.1298	1500	2.1056E-07	6.9031E-06	3.4109E-07	96.95	38.27
1.1298	2500	1.4343E-06	3.3642E-05	1.1315E-05	95.74	87.32
				Average:	94.20%	54,82%

From all the summarized tables 1-4, the histogram data was plotted to distinguish the coefficient value for each bearing case after applying the I-kaz^{TM} and I-kaz 3D analysis as in Figure 18 (a)-(d). Based on this analysis, gives the message that a faulty bearing condition can be detected by using the I-kaz^{TM} and I-kaz 3D analysis techniques. From the I-kaz representations or 3D scattering plot, it's were clearly show that there are remarkable differences between a good bearing scattering pattern with the other two defect bearing pattern signal which are the inner race fault and outer race fault. These defect bearing patterns showed more significance compared to the good bearing when the speed of the rotor frequency was regulated to the higher rpm. The difference parameter of load torque imposed on the bearing also give a small change between the pattern as compared to the speed variation parameter.

As mentioned previously, the I-kaz^{TM} and I-kaz 3D algorithm gives 2 outputs which are first the three-dimensional graphic display and second the I-kaz coefficient value that can be compared to the existing statistical parameter. By referring to Figure 18(a)-(d), all histograms were plotted from the value of I-kaz coefficients according to its specific study parameter, especially in speed variations. The trend shows that the I-kaz coefficients value is much higher when a larger amount of speed and load torque was applied to the bearing of the motor. In addition, it clearly shows that the inner race bearing defect can be successfully detected by the I-kaz 3D and I-kaz^{TM} at X-axis. However, for the outer race defect bearing can be detected by I-kaz 3D and I-kaz^{TM} from the Y-axis signal acquisition. The I-kaz^{TM} signal acquired from the Z-axis has less deviation average compared to I-kaz 3D, I-kaz^{TM} X-axis and Y-axis. The deviation signal average for all the techniques as shown in Table 1-4 indicated that the I-kaz^{TM} X-axis gives an excellent average deviation percentage of 96.86% in detecting the IRF defect bearing. It is followed by I-kaz 3D, I-kaz^{TM} Y-axis and I-kaz^{TM} Z-axis with average deviation percentages of 94.20%, 79.69%, and 57.06% respectively. However, the average deviation percentage between the outer race defect and good bearing was showing that the I-kaz^{TM} Y-axis is taking the lead by 65.4% and followed by I-kaz 3D, I-kaz^{TM} Z-axis, and I-kaz^{TM} X-axis with the percentages of 54.82%, 36.71%, and 22.91% respectively. The results show that the vibration-based monitoring method using I-kaz^{TM} and I-kaz 3D techniques is effective in detecting the faults in the bearing, especially in inner race cases.

4. Conclusions

These findings support the conclusion that a faulty bearing condition can be detected by using the I-kaz^{TM} and I-kaz 3D analysis techniques. The results analysis shows that the algorithm detection by I-kaz^{TM} gave higher deviation percentage average results (96.86%) compared to the I-kaz 3D (94.20%). By utilizing only, a single input vibration source, I-kaz^{TM} can give reliable output data by its coefficient value and three-dimensional scattering display. Compared to the I-kaz 3D, it needs three different input sources to validate the output analysis. Through this analysis, the I-kaz^{TM}

coefficient from Inner race fault (IRF) bearing gives a significant value compared to the Outer race fault (ORF). The results from this can conclude that the IRF can be accurately detected compared to the ORF case.

Acknowledgement

The author would like to thanks to Universiti Kuala Lumpur for supported this research by the Short-Term Research Grant (STRG) fund no. STR20007.

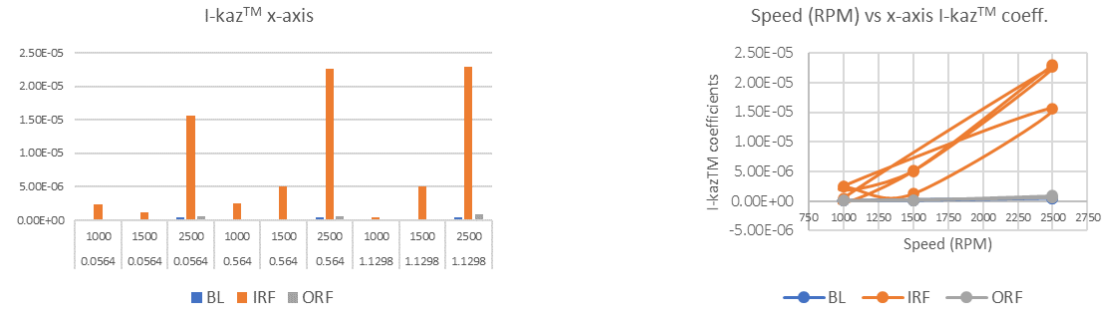

(a)

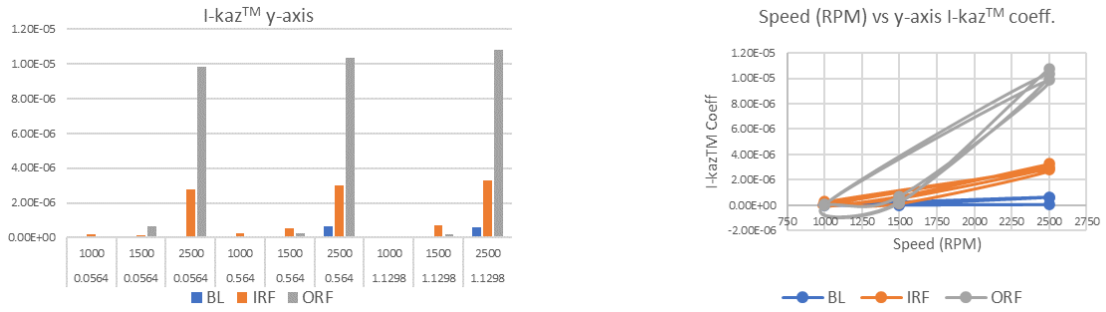

(b)

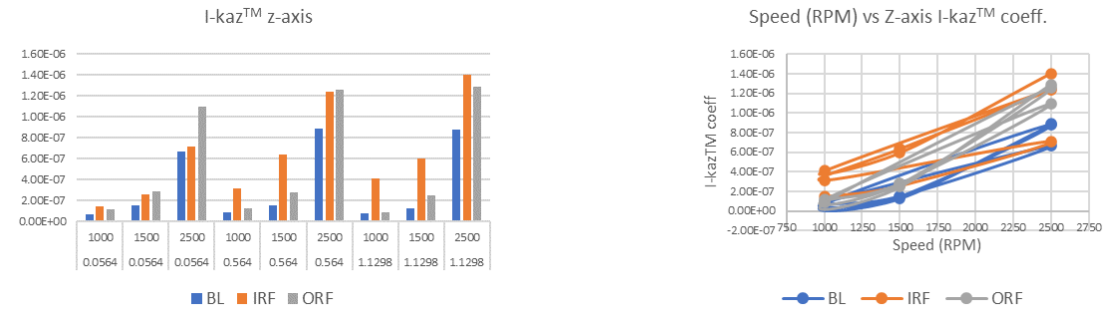

(c)

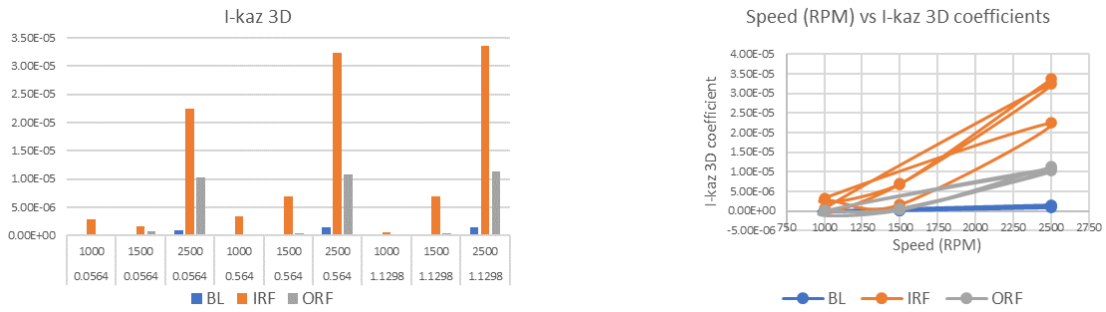

(d)

Fig. 18 - The histogram plot of I-kaz™ coefficient (a)X-axis; (b)Y-axis; (c)Z-axis, and; (d) I-kaz 3D

References

[1] A. V Dube, L. S. Dhamande, and P. G. Kulkarni, "Vibration Based Condition Assessment Of Rollingelement Bearings With Localized Defects," *Int. J. Sci. Technol. Res.*, vol. 2, no. 4, pp. 149-155, 2013, [Online]. Available: www.ijstr.org.

[2] M. Tiboni, C. Remino, R. Bussola, and C. Amici, "A Review on Vibration-Based Condition Monitoring of Rotating Machinery," *Appl. Sci.*, vol. 12, no. 3, 2022, doi: 10.3390/app12030972.

[3] N. R. Dreher, I. O. de Almeida, G. C. Storti, G. B. Daniel, and T. H. Machado, "Feature analysis by k-means clustering for damage assessment in rotating machinery with rolling bearings," *J. Brazilian Soc. Mech. Sci. Eng.*, vol. 44, no. 8, pp. 1-14, 2022, doi: 10.1007/s40430-022-03637-1.

[4] N. A. Kasim, M. G. Mohamed, and M. Z. Nuawi, "Non-Stationary Vibratory Signatures Bearing Fault Detection Using Alternative Novel Kurtosis-based Statistical Analysis," *J. Appl. Sci. Process Eng.*, vol. 9, no. 1, pp. 1139-1148, 2022, doi: 10.33736/jaspe.4594.2022.

[5] Z. Karim, M. Z. Nuawi, J. A. Ghani, S. Abdullah, and M. J. Ghazali, "Optimization of integrated kurtosis-based algorithm for Z-filter (I-kaz^{TM}) coefficient using multi level signal decomposition technique," *World Appl. Sci. J.*, vol. 14, no. 10, 2011.

[6] M. Z. Nuawi, M. J. M. Nor, N. Jamaludin, S. Abdullah, F. Lamin, and C. K. E. Nizwan, "Development of integrated Kurtosis-based Algorithm for Z-filter technique," *Journal of Applied Sciences*, vol. 8, no. 8. pp. 1541-1547, 2008, doi: 10.3923/jas.2008.1541.1547.

[7] M. Z. Nuawi, S. Abdullah, A. R. Ismail, and N. F. Kamaruddin, "A Novel Analysis (I-KAZ 3D) for Three Axial Vibration Signal in Bearing Condition Monitoring," *7th WSEAS Int. Conf. Syst. Sci. Simul. Eng. (ICOSSSE '08)*, no. November 2015, pp. 318-322, 2008.

[8] S. A. A. Aziz, M. Z. Nuawi, M. J. M. Nor, and D. D. I. Daruis, "Study of noise exposure inside a malaysian army three-tonne truck driver's compartment using I-KAZ^{TM}," *Def. S T Tech. Bull.*, vol. 7, no. 2, 2014.